Wind farms providing secondary frequency regulation: Evaluating the performance of model-based receding horizon control

2016 J. Phys.: Conf. Ser. 753 052012

(http://iopscience.iop.org/1742-6596/753/5/052012)

Wind farms providing secondary frequency regulation: Evaluating the performance of model-based receding horizon control

Carl R. Shapiro[1], Johan Meyers[2], Charles Meneveau[1], and Dennice F. Gayme[1]

[1] Department of Mechanical Engineering, Johns Hopkins University, Baltimore Maryland 21218, USA
[2] Department of Mechanical Engineering, KU Leuven, Celestijnenlaan 300A, 3001 Leuven, Belgium

E-mail: crshapiro@jhu.edu

Abstract. We investigate the use of wind farms to provide secondary frequency regulation for a power grid. Our approach uses model-based receding horizon control of a wind farm that is tested using a large eddy simulation (LES) framework. In order to enable real-time implementation, the control actions are computed based on a time-varying one-dimensional wake model. This model describes wake advection and interactions, both of which play an important role in wind farm power production. This controller is implemented in an LES model of an 84-turbine wind farm represented by actuator disk turbine models. Differences between the velocities at each turbine predicted by the wake model and measured in LES are used for closed-loop feedback. The controller is tested on two types of regulation signals, "RegA" and "RegD", obtained from PJM, an independent system operator in the eastern United States. Composite performance scores, which are used by PJM to qualify plants for regulation, are used to evaluate the performance of the controlled wind farm. Our results demonstrate that the controlled wind farm consistently performs well, passing the qualification threshold for all fast-acting RegD signals. For the RegA signal, which changes over slower time scales, the controlled wind farm's average performance surpasses the threshold, but further work is needed to enable the controlled system to achieve qualifying performance all of the time.

1. Introduction

Recent market trends are rapidly changing the composition of power grid energy resources, replacing conventional dispatchable power sources with variable resources like wind energy. These changes are putting pressure on the power system by reducing participation in services traditionally provided by dispatchable power sources [1]. A particularly important example is grid frequency regulation, which is closely tied to short-term imbalances in active power generation and load over time-scales ranging from miliseconds to tens of minutes [2]. In fact, a number of independent system operators (ISOs) are beginning to consider requiring wind plants to provide frequency regulation services and expanding frequency regulation markets to include wind plants [1, 3].

Secondary frequency regulation, where participating generators track a power signal sent by the ISO over tens of minutes, is an area of growing interest. Recent work [4, 5] has

shown that wind turbines can effectively provide secondary frequency regulation by reducing their operating power production setpoint to allow turbines to increase production levels while following the regulation signal. In previous studies [4, 5] individual turbine controllers required setpoint reductions that were exactly equal to the maximum increase of the regulation signal. However, this approach has two notable limitations. First, by reducing the power setpoint, wind turbines are sacrificing revenue in bulk energy markets to provide regulation, which may not be economically prudent [6]. Second, this approach cannot be directly extended to large wind farms because the time scales of the regulation signals are large enough that aerodynamic interactions between turbines become important. As such, single turbine control strategies that do not take into account these interactions can lead to unintended behavior. Approaches to overcome these challenges are just beginning to be explored [7–9].

Our recent work sought to overcome these challenges through the use of coordinated model-based receding-horizon control of an array of wind turbines to provide secondary frequency regulation [9]. Our approach first extends the classic Jensen model [10] to describe the effect of time-varying changes in a turbine's thrust coefficient on its wake. This time-varying wake model is subsequently used in the receding horizon controller, where the power tracking problem is iteratively solved by minimizing a cost function. Feedback is included by correcting model errors using measurements of the velocity at each turbine. This approach showed promising results when tested in a large eddy simulation (LES) model of a wind farm where turbines are represented using the actuator disk model. In these simulations, we used setpoint reductions of only 50% of the maximum regulation provided, which is more aggressive than previous single turbine approaches. Given the wind farm test system used and the initial conditions considered, the controller was able to track a regulation signal with these lower power setpoint reductions.

In this paper we further characterize the performance of the model-based receding horizon wind farm controller using regulation test signals and evaluation criteria from PJM, an ISO in the United States Eastern Interconnection [11, 12]. PJM implements secondary frequency regulation through two regulation signals. These signals are low and high pass filters of the Area Control Error (ACE), a combined measure of the power imbalance and deviation of the frequency from its nominal operating value. The "RegA" signal is a low pass filter of the ACE that is generally followed using traditional regulating resources, such as fossil fuel plants. The "RegD" signal is a high pass filter of the ACE that can be followed by more quickly responding resources, such as energy storage devices.

In order to participate in PJM's regulation market, power plants must pass the Regulation Qualification Test for each type of regulation signal the plant wishes to provide. This test is performed over a 40-minute period, and tested resources must follow a simulated regulation signal sent by PJM. Performance is quantified using a composite performance score, which is the weighted sum of a delay, correlation, and precision score. The accuracy score measures the ability of the signal to respond to a change in the ISO regulation signal. The delay score measures the delay in the plant's response to the regulation signal. The precision score measures the difference between the requested power and the plant's power output. A minimum score of 75% is needed to qualify to participate in each of the two regulation services. This performance score is also used to continuously evaluate participating generators. If a participating plant's average score over the last 100 hours drops below 40%, then the plant is disqualified from providing the particular service and must retake the initial performance test to requalify.

In this work we study the ability of our controlled wind farm to meet PJM's performance score metrics for both regulation signal types. In lieu of a real wind farm, a LES framework with actuator disk turbine models is used as a 'model wind farm' to test the controller. These simulations allow us to determine whether wind farms with this strategy are better suited to provide traditional (RegA) or fast-acting (RegD) regulation. The remainder of this paper is organized as follows. Section 2 discusses the controller strategy and underlying wake model.

Section 3 describes the test cases. Section 4 presents and discusses the results. Section 5 gives conclusions and discusses directions for future work.

2. Methods

We use the previously developed [9] model-based receding horizon control framework that results in the controlled system shown in Figure 1. As in typical receding horizon approaches [13, 14], the control action is computed for a long time period compared to the relevant dynamics of the system. The computed control signal is then implemented for a fraction of that time, after which the current state of the system is measured and used to initialize a new control computation. Each control action is computed based on a reference signal $P_{\text{ref}}(t)$. The receding horizon control algorithm computes a control trajectory based on the time-varying wake model. The control actions are implemented through the local thrust coefficients $\mathbf{C}'_T(t)$, which are sent to each row of turbines in the LES model wind farm. Closed-loop feedback is incorporated by measuring the difference between the measured wind speed $\mathbf{u}(t)$ and the estimated wind speed $\hat{\mathbf{u}}(t)$ at each row of turbines. The difference between the two velocities is passed through an error correction filter that updates the estimates used in the next control computation through the error correction term $\boldsymbol{\epsilon}(t)$. The next sections describe the controller and plants blocks in Figure 1 in more detail.

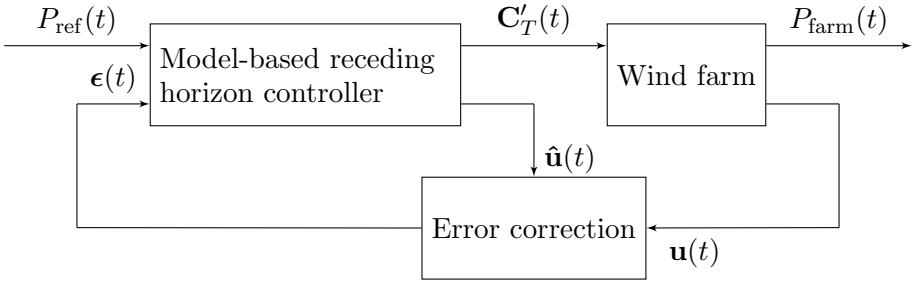

Figure 1. Controlled wind farm system block diagram showing the model-based receding horizon controller and wind farm.

2.1. Wind farm test system

The controller is tested in a LES model of a wind farm with wind turbines represented using actuator disk models. The wind farm is composed of N rows of M aligned turbines. Each turbine has a 100 m rotor diameter D and a 100 m hub height. The spacing between turbines is $7D$ in the streamwise direction and $5D$ in the spanwise direction. Prior to initiation of the control, the turbines are operated at a constant local thrust coefficient of $C'_T = 1.33$, which is meant to be representative of standard wind turbine operating conditions [15]. These simulations are performed using JHU's LESGO code [15–17], which uses pseudo-spectral discretization in the horizontal directions with periodic boundary conditions. Second-order Adams-Bashforth time integration, second-order finite differencing in the vertical direction, and the dynamic scale-dependent Lagrangian Smagorinsky subgrid stress model [18] are used. Inlet conditions for the wind farm are generated using the concurrent-precursor method [17]. An instantaneous color contour plot of the streamwise velocity field from one of these simulations is shown in Figure 2.

2.2. Wake model

At the heart of the model-based receding-horizon controller is a one-dimensional time-varying wake model that has been validated against LES of wind farms at startup [9]. This model follows the approach of the classic Jensen model [10] by first computing the wake deficit velocity $\delta u_n(x,t)$

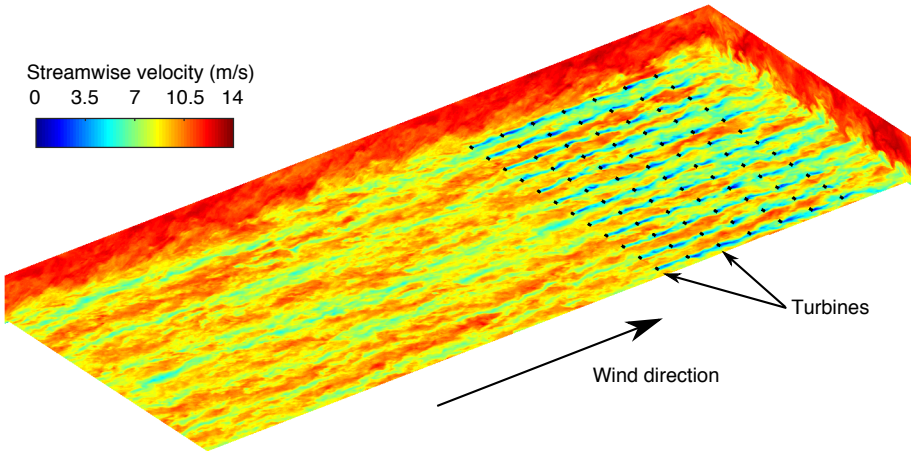

Figure 2. Instantaneous streamwise velocity contours for a large eddy simulation with actuator disk turbine models, which are indicated by black lines.

for each turbine n as if each turbine was on its own (with the same freestream velocity U_∞) and subsequently superposing the velocity deficits using the common "square-superposition" approach [10]. Time-dependency is included by allowing the local thrust coefficients $\mathbf{C}'_T(t)$ to vary in time.

Assuming the wake travels with the freestream velocity U_∞ and reducing the spatial dimension to the streamwise direction by considering rows of turbines collectively, it was shown in [9] that the velocity deficit is governed by

$$\frac{\partial \delta u_n}{\partial t} + U_\infty \frac{\partial \delta u_n}{\partial x} = -w_n(x)\delta u_n(x,t) + f_n(x,t), \tag{1}$$

where $w_n(x)$ is the wake decay function and $f_n(x,t)$ is the forcing function used to account for the effect of the turbine on the flow field. The wake decay function

$$w_n(x) = 2\frac{U_\infty}{d_n(x)}\frac{d}{dx}d_n(x) \tag{2}$$

is determined by assuming that the wake diameter normalized by the rotor diameter $d_n(x)$ at a fixed location x is constant in time. Momentum theory shows that as the air flows through the turbine rotor, the velocity reduces to $U_\infty - 2U_\infty C'_{Tn}/(4 + C'_{Tn})$ [9]. In order to retrieve this expected velocity reduction, the forcing function is specified as

$$f_n(x,t) = \frac{2U_\infty^2}{d_n^2(x)}\frac{C'_{Tn}(t)}{4 + C'_{Tn}(t)}G(x - s_n), \tag{3}$$

where $G(x - s_n)$ is a function that integrates to unity, centered at the streamwise location of the turbine $x = s_n$. A Gaussian function with characteristic width Δ

$$G(x - s_n) = \frac{1}{\Delta\sqrt{2\pi}}e^{-\frac{(x-s_n)^2}{2\Delta^2}} \tag{4}$$

maintains smoothness in the velocity deficit fields.

Furthermore, we specify the normalized wake diameter $d_n(x)$ using a modified version of the Jensen model [10]. In the Jensen model, the dimensionless diameter of the wake generated by

turbine row n is $d_n(x) = 1+2k_n(x-s_n)/D$, where k_n is an empirical wake expansion coefficient. We make two modifications to this equation. First, the linear expansion is assumed to begin at $x = s_n+2\Delta$ to prevent the wake expansion from occurring within the induction zone imposed by the Gaussian forcing. Second, the equation for the standard Jensen dimensionless wake diameter is ill-posed upstream of the turbine, where it can vanish or become negative. Therefore, we instead use the following modified function that smoothly approximates the linear expansion in the far wake while avoiding becoming less than unity close to the turbine

$$d_n(x) = 1 + k_n \ln\left[1 + \exp\left(\frac{x - s_n - 2\Delta}{D/2}\right)\right]. \tag{5}$$

The squared deficits [10] are superposed to calculate the estimated streamwise velocity $\hat{u}_n$ at the turbine

$$\hat{u}_n(t) = U_\infty - \int_0^L \left(\sum_{m=1}^{N} \delta u_m^2(x,t)\right)^{1/2} G(x - s_n)\, dx. \tag{6}$$

Finally, the total estimated power $\hat{P}_n$ of the M turbines in row n is

$$\hat{P}_n = M\frac{1}{2}\rho\frac{\pi D^2}{4}C'_{Tn}\hat{u}_n^3, \tag{7}$$

where the local power coefficient is approximated by the local thrust coefficient $C'_P = C'_T$ [14].

2.3. Controller design

The controller is implemented using the model-based receding horizon framework introduced in [9]. The receding horizon method works by iteratively solving a finite-time minimization problem over a time horizon T. The solution is implemented for a shorter period T_A before re-solving the minimization problem. More details about this procedure can be found in [13, 14].

In order to apply this method, the secondary frequency regulation problem is rewritten as the following minimization of a cost functional $\mathscr{J}$ constrained by the time-varying wake model $\mathbf{W}(\mathbf{C}'_T, \mathbf{q}) = 0$.

$$\underset{\mathbf{C}'_T, \mathbf{q}}{\text{minimize}} \qquad \mathscr{J}(\mathbf{C}'_T, \mathbf{q}) \tag{8}$$

$$\text{subject to} \qquad \mathbf{W}(\mathbf{C}'_T, \mathbf{q}) = 0, \tag{9}$$

where the vector of local thrust coefficients for each row of turbines $\mathbf{C}'_T$ are the control variables and $\mathbf{q} = [\boldsymbol{\delta}\mathbf{u}, \hat{\mathbf{u}}]$ are the states of the wake model discussed in Section 2.2. In this work we use the cost functional

$$\mathscr{J} = \frac{1}{\mathscr{P}^2 T}\int_0^T \left(\sum_{n=1}^{N} \hat{P}_n(t) - P_{\text{ref}}(t)\right)^2 dt + \mathscr{R} \tag{10}$$

that describes the reference tracking goal and regularizations $\mathscr{R}$ to produce well behaved results. The constant $\mathscr{P}$ normalizes the power of each row of M turbines, and the time T is the finite time period considered. The regularizations chosen are

$$\mathscr{R} = \frac{\eta}{T}\sum_{n=1}^{N}\int_0^T \left(C'_{Tn}(t) - C'_{T\text{ref}}\right)^2 dt + \gamma T \sum_{n=1}^{N}\int_0^T \left(\frac{dC'_{Tn}}{dt}\right)^2 dt, \tag{11}$$

where the first term penalizes deviations away from the pre-control thrust coefficient $C'_{T\text{ref}}$ and the second term penalizes large time derivatives of the thrust coefficients to prevent high

frequency oscillations in the control. The constants γ and η are the weights of each regularization term.

Closed-loop feedback is provided by an exponentially-decaying error correction term $\boldsymbol{\epsilon}$ that is added to the velocity estimate $\hat{\mathbf{u}}$. The error correction for turbine n at the iteration starting at time t_c is $\epsilon_n(t) = (u_n(t_c) - \hat{u}_n(t_c))\, e^{-(t-t_c)/\tau}$, where $u_n(t_c)$ is the current velocity measurement at the turbine from the LES and $\hat{u}_n(t_c)$ is the current velocity estimate from the wake model. Turbine velocities are measured indirectly using measured total power generated by each row and the local thrust coefficient. The error correction has a time constant of τ =120 s.

For each iteration of the receding horizon controller, the power tracking problem is solved by minimizing the modified unconstrained reduced cost functional $\tilde{\mathscr{J}}(\mathbf{C}'_T) = \mathscr{J}(\mathbf{q}, \mathbf{C}'_T)$ [13, 14]. The minimization uses the gradient-based nonlinear Polak-Ribière conjugate gradient method [19] combined with the Moré-Thuente line search method [20]. Gradients are obtained using one backward simulation of the adjoint equations of the wake model (shown in more detail in [9]) using the the formal Lagrangian method [14, 21]. Minimizations are terminated after 100 iterations.

3. Test cases

The performance of the controlled wind farm is tested using eight signals made up of PJM's published RegA and RegD test signals as well as historical RegA and RegD signals from three randomly selected hours in 2015 [22]. For each regulation signal, we examined three initial conditions and two levels of power setpoint reduction, which we also refer to as derates. For each controller test, the reference signal is defined as $P_{\text{ref}}(t) = [1 - \alpha + 0.08r(t)]P_{\text{base}}$. The baseline power P_{base} is defined as the 5-minute average power prior to initiation of the control, the derate amount is defined as α, and the regulation signal from the ISO is $r(t) \in [-1, 1]$ such that the reference signal varies by $\pm 8\%$ of P_{base}. The historical signals are the hours starting at: 3 pm on Februrary 14, 2015; 8 pm on August 17, 2015; and 10 am on November 28, 2015.

A total of 48 test cases are used through a combination of the four variables discussed above. Each test case is given a unique identifier that is a combination of identifiers for each of the variable types shown in Table 1."Signal" refers to the regulation signal type (RegA or RegD), "Derate" refers the to derate amount (4 or 6%), "Initial condition" refers to the initial condition of the controlled plant simulation, and "Period" refers to the regulation signal period, which is either the PJM test signals or a randomly selected hour in 2015. For example, the test case "RegA.D4.IC1.TS" refers to the case with the RegA test signal, 4% derate, and the first initial condition.

4. Results and discussion

The time evolution of the total farm power in LES are compared to the reference signals for initial condition 3 and a 4% derate in Figure 3, showing all regulation signals (RegA or RegD) and regulation period combinations. These results demonstrate the good overall tracking performance of the controlled wind farm, except for a few specific periods of under-performance. Furthermore, the results demonstrate that this control method is also able to reduce the natural turbulent fluctuations in power production of the wind farm. Quantitative measures of the performance of each regulation signal type (RegA or RegD) and derate value (4% and 6%) combination are shown in terms of PJM's performance scores in Figure 4. The controlled wind farm performs better for the RegD signals, meeting the composite score threshold for qualification of 75% in all cases. The performance of the RegA signals is also satisfactory for PJM participation, but the controller would not have qualified in all tests. However, in cases

Table 1. Test case identifiers

Identifier	Type	Description
RegA	Signal	Traditional RegA regulation signal
RegD	Signal	Fast-responding RegD regulation signal
D4	Derate	Power setpoint is reduced by 4% of P_{base}
D6	Derate	Power setpoint is reduced by 6% of P_{base}
IC1	Initial condition	Initial condition 1
IC2	Initial condition	Initial condition 2
IC3	Initial condition	Initial condition 3
TS	Period	Test signals
H1	Period	Februrary 14, 2015 at 3 pm
H2	Period	August 17, 2015 at 8 pm
H3	Period	November 28, 2015 at 10 am

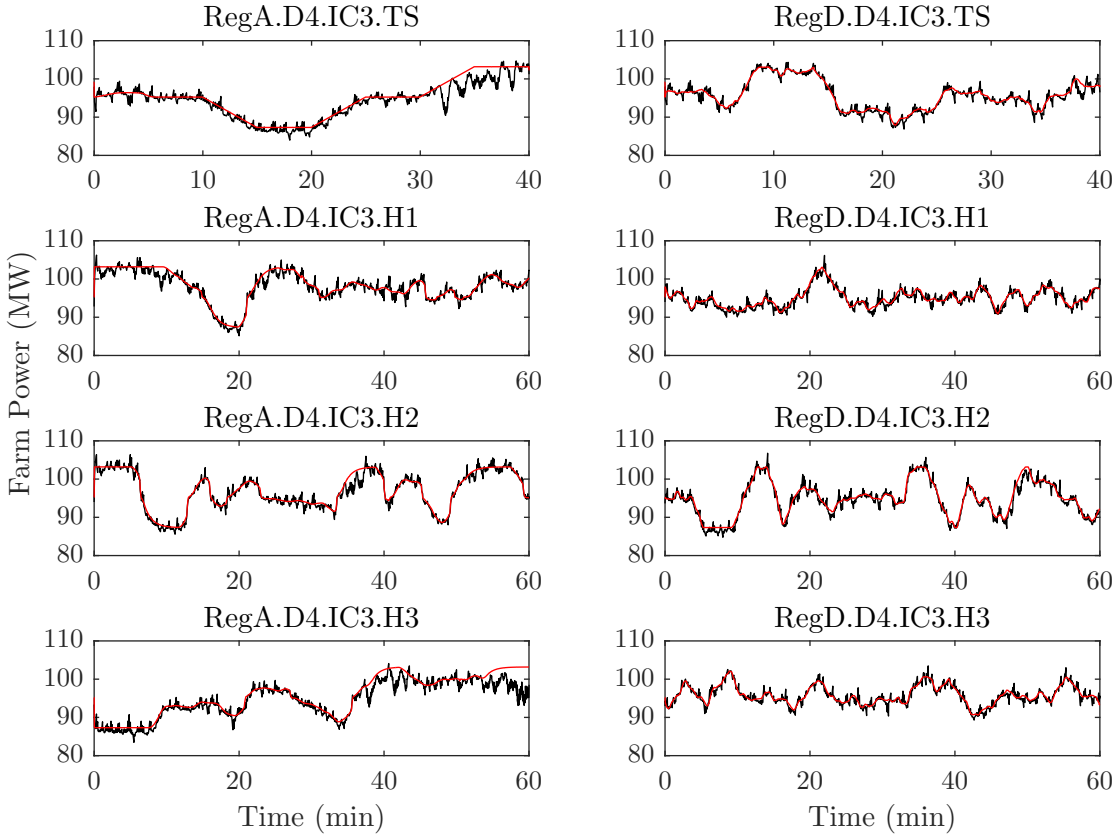

Figure 3. Comparison of simulated farm power from controlled LES wind farm model (——) and power reference signals (——) for 4% derate and initial condition 3.

where the controlled wind farm had poor performance for the RegA signal with 4% derate, increasing the derate to 6% markedly improved the overall performance.

These results provide important insights into the possible strengths and limitations of the proposed approach to wind farm control for frequency regulation. First, these results suggest

that wind farms may be better suited to act as a quickly responding resource for grid regulation services. The consistently passing composite performance score for the RegD signals indicates that these controlled wind farms are able to provide this service reliably. Further work, however, is needed to improve the performance of the method in providing slower regulation services. The lower RegA scores are partially explained by the controlled wind farm's inability to provide prolonged periods of up-regulation, such during the last 10 minutes of the "RegA.D4.IC3.TS" and "RegA.D4.IC3.H3" cases. Future work is needed to determine whether this is a fundamental limitation of the wind farm dynamics or the control strategy.

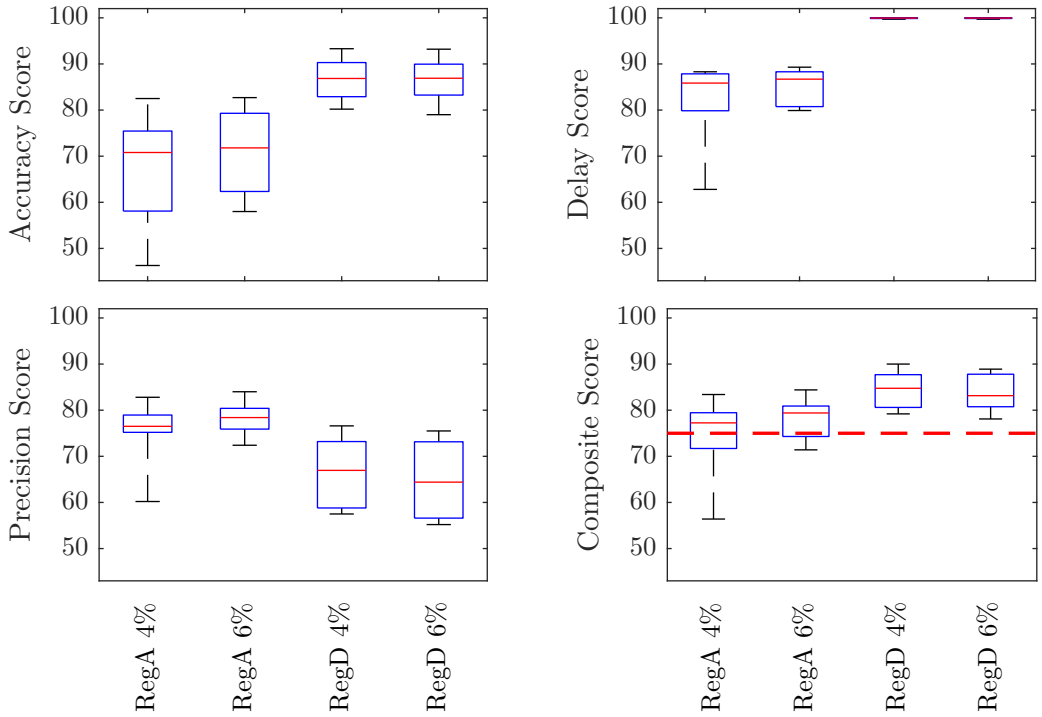

Figure 4. Boxplots of PJM performance scores for all regulation signal type (RegA or RegD) and derate value (4% and 6%) combinations. The qualification threshold of 75% for the composite score (— — —) is shown in the lower right panel.

The power tracking results in Figure 3 demonstrate that the controller is able to track the up-regulation portions of the RegA signals at the beginning of the control period, such as during the first 5–10 minutes of the signals on 2/14 and 8/17. However, when up-regulation is requested towards the end of the control interval, such as the test signal and the signal on 11/28, the controller does not perform as well. A possible explanation is that the available energy in the wind is slowly changing as the atmospheric boundary layer evolves. Since estimates of available energy are readily available over short time horizons, more frequent market clearing may allow wind farms to more effectively provide regulation.

5. Conclusion and future work

In this study we further demonstrate the effectiveness of the model-based receding horizon control strategy for wind farms providing secondary frequency regulation. The tracking performance of the controlled wind farm is quantified using PJM's performance metrics. All

fast-regulation RegD scores exceed the PJM threshold for regulation participation. However, more work is needed to allow the controlled wind farm to consistently exceed the threshold for the RegA signals. These results indicate that this model-based receding horizon controller design could allow wind farms to meet industry design standards and allow wind farms to fully participate in regulation markets, particularly in fast-acting regulation markets.

The potential for reducing the derate required to participate in these regulation markets was also explored. Participating in frequency regulation markets currently requires a trade-off between revenue losses in the bulk power market and revenues generated in the frequency market. Previous approaches [4, 5] required power setpoint reductions of an amount equal to the regulation amount, which directly reduces bulk power revenue by this amount. For this study we took a more aggressive approach by reducing the power setpoint by only 75%, and even only 50%, of the maximum regulation provided. For both of these derates, the controller is able to track fast-acting RegD signals. The potential for reducing the required derate has important economic implications for wind farms participating in both energy and regulation markets, a situation that will become increasingly common as more ISOs require wind farms to contribute to this grid service.

Although the controller design showed promising results, more work is needed to push this approach towards the implementation phase. We used the local thrust coefficient as a surrogate for real turbine control variables, such as generator torque and blade pitch angle. Improvements to our representation of these variables through actuator line methods and the inclusion of drivetrain dynamics in the control method are needed. Including rotational inertia may allow for further reductions in the amount of derate because rotational kinetic energy can compensate for short term power shortages [23]. Furthermore, we assumed that the ISO provided the regulation signal at the beginning of the control period; however, PJM provides this reference at a 2 second scan rate. This shortcoming could be addressed by adding estimated reference trajectories to the control design.

Acknowledgements

CRS, CM, and DFG are supported by the National Science Foundation (grant nos: ECCS-1230788 and OISE-1243482, the WINDINSPIRE project). JM is supported by the European Research Council (ActiveWindFarms, grant no: 306471). This research project was conducted using computational resources at the Maryland Advanced Research Computing Center (MARCC).

References

[1] Aho J, Buckspan A, Laks J, Fleming P, Jeong Y, Dunne F, Churchfield M, Pao L and Johnson K 2012 A tutorial of wind turbine control for supporting grid frequency through active power control *American Control Conference* pp 3120–3131

[2] Rebours Y, Kirschen D, Trotignon M and Rossignol S 2007 A survey of frequency and voltage control ancillary services—Part I: Technical features *IEEE Transactions on Power Systems* **22** 350–357

[3] Díaz-González F, Hau M, Sumper A and Gomis-Bellmunt O 2014 Participation of wind power plants in system frequency control: Review of grid code requirements and control methods *Renewable and Sustainable Energy Reviews* **34** 551–564

[4] Aho J, Buckspan A, Pao L, Fleming P *et al.* 2013 An active power control system for wind turbines capable of primary and secondary frequency control for supporting grid reliability *AIAA Aerospace Sciences Meeting*

[5] Jeong Y, Johnson K and Fleming P 2014 Comparison and testing of power reserve control strategies for grid-connected wind turbines *Wind Energy* **17** 343–358

[6] Rose S and Apt J 2014 The cost of curtailing wind turbines for secondary frequency regulation capacity *Energy Systems* **5** 407–422

[7] Annoni J, Howard K, Seiler P and Guala M 2015 An experimental investigation on the effect of individual turbine control on wind farm dynamics *Wind Energy*

[8] Gebraad P M O, Fleming P A and van Wingerden J W 2015 Wind turbine wake estimation and control using FLORIDyn, a control-oriented dynamic wind plant model *American Control Conference* pp 1702–1708

[9] Shapiro C R, Bauweraerts P, Meyers J, Meneveau C and Dennice G F 2016 Model-based receding horizon control of wind farms for secondary frequency regulation *Wind Energy* **Submitted**
[10] Katić I, Højstrup J and Jensen N 1986 A simple model for cluster efficiency *European Wind Energy Association Conference and Exhibition* pp 407–410
[11] PJM 2012 *PJM Manual 11: Energy & Ancillary Services Market Operations*
[12] PJM 2015 *PJM Manual 12: Balancing Operations*
[13] Bewley T R, Moin P and Temam R 2001 DNS-based predictive control of turbulence: An optimal benchmark for feedback algorithms *Journal of Fluid Mechanics* **447** 179–225
[14] Goit J P and Meyers J 2015 Optimal control of energy extraction in wind-farm boundary layers *Journal of Fluid Mechanics* **768** 5–50
[15] Calaf M, Meneveau C and Meyers J 2010 Large eddy simulation study of fully developed wind-turbine array boundary layers *Physics of Fluids* **22**
[16] VerHulst C and Meneveau C 2015 Altering kinetic energy entrainment in large eddy simulations of large wind farms using unconventional wind turbine actuator forcing *Energies* **8** 370–386
[17] Stevens R J A M, Graham J and Meneveau C 2014 A concurrent precursor inflow method for large eddy simulations and applications to finite length wind farms *Renewable Energy* **68** 46–50
[18] Bou-Zeid E, Meneveau C and Parlange M 2005 A scale-dependent Lagrangian dynamic model for large eddy simulation of complex turbulent flows *Physics of Fluids* **17**
[19] Press W H 2007 *Numerical recipes 3rd edition: The art of scientific computing* (Cambridge University Press)
[20] Moré J J and Thuente D J 1994 Line search algorithms with guaranteed sufficient decrease *ACM Transactions on Mathematical Software* **20** 286–307
[21] Borzì A and Schulz V 2011 *Computational Optimization of Systems Governed by Partial Differential Equations* (SIAM)
[22] PJM Ancillary services URL `http://www.pjm.com/markets-and-operations/ancillary-services.aspx`
[23] De Rijcke S, Driesen J and Meyers J 2015 Power smoothing in large wind farms using optimal control of rotating kinetic energy reserves *Wind Energy* **18** 1777–1791